Journal of Experimental Botany, Vol. 62, No. 1, pp. 331–343, 2011
doi:10.1093/jxb/erq279 Advance Access publication 11 October, 2010

Journal of Experimental Botany
www.jxb.oxfordjournals.org

RESEARCH PAPER

Mechanistic study of mitochondria-dependent programmed cell death induced by aluminium phytotoxicity using fluorescence techniques

Zhe Li and Da Xing*

MOE Key Laboratory of Laser Life Science and Institute of Laser Life Science, College of Biophotonics, South China Normal University, Guangzhou 510631, China

* To whom correspondence should be addressed: E-mail: xingda@scnu.edu.cn

Received 22 May 2010; Revised 12 July 2010; Accepted 19 August 2010

Abstract

Recent studies have suggested that aluminium (Al) induces programmed cell death (PCD) in plants. To investigate possible mechanisms, fluorescence techniques were used to monitor the behaviour of mitochondria *in vivo*, as well as the activation of caspase-3-like activity during protoplast PCD induced by Al. A quick burst of mitochondrial reactive oxygen species (ROS) was detected in Al-treated protoplasts. The mitochondrial swelling and mitochondrial transmembrane potential (MTP) loss occurred prior to cell death. Pre-incubation with ascorbic acid (AsA, antioxidant molecule) retarded mitochondrial swelling and MTP loss. The real-time detection of caspase-3-like activation was achieved by measuring the degree of fluorescence resonance energy transfer (FRET). At 30 min after exposure to Al, caspase-3-like protease activation, indicated by the decrease in the FRET ratio, occurred, taking about 1 h to reach completion in single living protoplasts. The mitochondrial permeability transition pore (MPTP) inhibitor, cyclosporine (CsA) gave significant protection against MTP loss and subsequent caspase-3-like activation. Our data also showed that Al-induced mitochondrial ROS possibly originated from complex I and III damage in the respiratory chain through the interaction between Al and iron-sulphur (Fe–S) protein. Alternative oxidase (AOX), the unique respiratory terminal oxidase in plants, was demonstrated to play protective roles in Al-induced protoplast death. Our results showed that mitochondrial swelling and MTP loss, as well as the generation of mitochondrial ROS play important roles in Al-induced caspase-3-like activation and PCD, which provided new insight into the signalling cascades that modulate Al phytotoxicity mechanism.

Key words: Alternative oxidase, aluminium, *Arabidopsis*, caspase-3-like, fluorescence techniques, mitochondria, programmed cell death, reactive oxygen species, respiratory chain.

Introduction

In plants, as in animals, cell death is a crucial process during development and the stress responses. The term programmed cell death (PCD) defines forms of cell death involving a series of orderly processes mediated by intracellular death programmes, regardless of the triggers or the hallmarks it exhibits (Van Breusegem and Dat, 2006; Zhang and Xing, 2008). PCD plays important roles to maintain the proper development and appropriate stress responses. Many dying plant cells undergo biochemical and morphological changes similar to those in apoptotic mammalian cells, including caspase-like activation, DNA fragmentation, and chromatin condensation (Danon *et al.*, 2000).

Intensive effort has been put into investigating the key factors that regulate PCD. Chloroplasts are important sites of ROS production and may generate intermediate

Abbreviations: AOX, alternative oxidase; AsA, ascorbic acid; CsA, cyclosporine A; FDA, fluorescein diacetate; FRET, Fluorescence resonance energy transfer; H_2DCFDA, 2', 7'-dichlorodihydrofluorescein diacetate; LCSM, laser confocal scanning microscope; MPTP, mitochondrial permeability transitions pore; MTP, mitochondrial transmembrane potential; PCD, programmed cell death; Rh123, rhodamine 123; ROS, reactive oxygen species.

stress signals involved in the stress response and PCD (Gao *et al.*, 2008; Zhang and Xing, 2008; Doyle *et al.*, 2010). Analysis of the *Arabidopsis* conditional fluorescence mutant has clearly demonstrated that $^1O_2$ generated from excess protochlorophyllide can function as a signal leading to cell death (Wagner *et al.*, 2004). As the common organelle in animals and plants, the mitochondrial behaviour, including redox status and physiological function, have gained wide attention (Simon *et al.*, 2000; Yao *et al.*, 2002; Jeffrey, 2006; Logan, 2006; Noctor *et al.*, 2006; Hiroko *et al.*, 2007; Mayank *et al.*, 2007; Orrenius *et al.*, 2007). In many forms of mammalian cell apoptosis, mitochondria integrate diverse cellular stress signals and initiate the death execution pathway. Mitochondrial transmembrane potential (MTP) loss caused by the opening of mitochondrial permeability transition pores (MPTP) (Jeffrey, 2006), release of cytochrome *c* localized in the mitochondrial intermembrane space, and the stimulation of caspase proteolytic activities, are key regulatory events that precede nuclear DNA fragmentation and other apoptotic hallmarks (Wang, 2001). In plant cells, either abiotic or biotic stresses can raise reactive oxygen species (ROS) levels due to perturbations of mitochondrial metabolism (Apel and Hirt, 2004). Recently, the involvement of mitochondria in plant PCD has been reported showing that mitochondrial oxidative burst or membrane potential changes are commonly involved in PCD of *Arabidopsis* under various environmental stresses (Yao *et al.*, 2004; Gao *et al.*, 2008; Zhang and Xing, 2008). In addition, the ROS-dependent release of cytochrome *c* from mitochondria is detected during heat shock-induced PCD in tobacco Bright-Yellow 2 cells (Vacca *et al.*, 2006). These findings indicate that mitochondrial function may be shared in a very similar way during PCD in both animals and plants.

Under adverse conditions, the formation of ROS at the mitochondria can be minimized by a number of antioxidant regulatory mechanisms including the alternative NADH dehydrogenases and alternative oxidase (AOX) (Noctor *et al.*, 2006; Orrenius *et al.*, 2007). AOX, the unique respiratory terminal oxidase in plants, catalyses the energy-wasteful alternative respiration pathway. Under the situation that electron transport in the cytochrome *c* pathway is blocked by stress, AOX helps to maintain the electron flux and to reduce mitochondrial ROS levels (Millenaar and Lambers, 2003; Plaxton and Podesta, 2006). AOX1a, an important member of the AOX family, is often dramatically induced at the transcript level by a variety of stresses (Millenaar and Lambers, 2003). Such flexibility in plant respiration is considered as an essential mechanism which makes plants adapt better to stress conditions.

Aluminium (Al), is a non-essential metal widespread in the environment that is known to be toxic to humans as well as to plants, causing damage not only to the roots that are always exposed to Al but also to the aerial parts of plants. Its toxicity has been recognized as one of the major factors that limit crop production on acid soil. In humans, Al is considered as a neurotoxic metal that is connected with the onset of neurodegenerative disorders by the induction of apoptosis (Ghribi *et al.*, 2002; Fu *et al.*, 2003). Recent researches have described some apoptosis-like characters upon Al treatment in plant cells including the appearance of the DNA ladder, changes in nucleus morphology, and the fragmentation of the nucleus (Panda *et al.*, 2008), and have determined the potential roles of anti-apoptotic members in Al tolerance (Yakimova *et al.*, 2007; Zheng *et al.*, 2007). Al toxicity in plants is also believed to be associated with oxidative damage and mitochondrial dysfunction (Keith *et al.*, 1998; Yamamoto *et al.*, 2002; Boscolo *et al.*, 2003; Panda *et al.*, 2008; Yin *et al.*, 2010). Although more attention has been paid to Al phytotoxicity research, a mechanistic analysis of cell death, including the oxidative damage and the impairment of organelles, is lacking in many studies.

Fluorescence resonance energy transfer (FRET) has been widely used to study protein–protein interactions in living cells. It can be effectively used to study cellular activities, such as caspase activation during cell apoptosis, with specifically designed genetic reporters. Our recent work (Zhang *et al.*, 2009) provides a FRET probe which has been successfully used to detect caspase-3-like protease activation in UV-stressed *Arabidopsis* protoplasts, making the *in vivo* detection of caspase-like activity in plant cells possible.

The aim of our present work is to elucidate some of the signalling events, and to assess the behaviour of mitochondria as well as the activation of caspase-3-like activity under Al treatment. Based on the results obtained from cell imaging and biochemical approaches, this work provides a new insight into the mitochondria-dependent mechanism of Al-induced *Arabidopsis* protoplast PCD.

Materials and methods

Plant materials and chemical reagents

Plants of wild-type *Arabidopsis* (ecotype Columbia; WT), transgenic *Arabidopsis* possessing mitochondria-localized GFP (Logan and Leaver, 2000) and *Arabidopsis* lacking (aox1a) or over-expressing (AOX1a-OE) the *AOX1a* gene (purchased from NASC) were grown in soil culture in a growth chamber (model E7/2; Conviron, Winnipeg, MB, Canada) with a 16 h light photoperiod (120 μmol quanta m^{-2} s^{-1}) and 82% relative humidity at 22 °C for 3–4 weeks.

2', 7'-Dichlorodihydrofluorescein diacetate (H_2DCFDA), rhodamine 123 (Rh123), MitoSOX Red, and MitoTracker Red CMXRos were obtained from Molecular Probes (Eugene, OR, USA). Fluorescein diacetate (FDA), ascorbic acid (AsA), and cyclosporine (CsA) were purchased from Sigma-Aldrich, China (Shanghai, China).

Isolation and transient transfection of Arabidopsis *mesophyll protoplasts*

The procedures were performed according to our previous study (Zhang *et al.*, 2009). Small leaf strips (0.5–1 mm) in the enzyme solution that included cellulase R10 and macerozyme R10 (Yakult Honsha, Tokyo, Japan) were vacuum-infiltrated for about 30 min and then incubated in the dark for 3 h. After filtration through

a 75 μm nylon mesh, the crude protoplast filtrates were sedimented by centrifugation for 3 min at 100 *g*. The purified protoplasts were suspended in W5 solution (154 mM NaCl, 125 mM $CaCl_2$, 5 mM KCl, 5 mM glucose, 1.5 mM MES-KOH, pH 5.6) and counted in a haemocytometer. Before transfection, the protoplasts in W5 solution were bathed in ice for 30 min, and the supernatant was removed. The protoplasts were resuspended in mannitol–$MgCl_2$ solution (0.4 M mannitol, 15 mM $MgCl_2$, and 4 mM MES pH 5.7) at room temperature, and the concentration was adjusted to about 2×10^5 protoplasts ml^{-1}. For transfection of the PI-ECFP-DEVD-EYFP plasmid, 100 ml of protoplasts in mannitol–$MgCl_2$ solution was incubated with 10–20 mg plasmid DNA and 120 ml of polyethylene glycol (PEG) solution [40% (w/v) PEG-4000, 0.2 M mannitol, and 0.1 M $CaCl_2$]. After incubation for 5–30 min at room temperature, 0.5 ml of W5 solution was added to stop the transfection. After centrifugation to remove the PEG solution, the protoplasts were collected and resuspended in 250 ml of W5 solution (24-well plates). Transfected protoplasts were left in the dark at room temperature for 8–20 h to allow the expression of the ECFP-DEVD-EYFP fusion protein.

Preparation of mitochondria protein, content of Fe–S protein, and activity of respiratory chain complexes

Mitochondria or mitochondrial proteins were isolated from protoplasts of 3-week-old *Arabidopsis* leaves, using the method described previously by Moller and Rasmusson (2005), and immediately used or stored at –80 °C. The content of Fe–S protein was measured using mitochondrial proteins as the change in absorbance in 400 nm (A400) (Roland and Ulrich, 2006). NADH dehydrogenase (complex I) and cytochrome reductase (complex III) activities were assayed with mitochondrial proteins using the activity detection kit for mitochondrial respiratory chain complex I and III according to the manufacturer's manual (GENMED, Shanghai, China).

Al application

To treat *Arabidopsis* protoplasts or isolated mitochondria, $AlCl_3$ solutions (pH 4.5) at the indicated concentrations were added to 100 μl of protoplasts or isolated mitochondria suspension in 96-well plates and incubated for the required time at room temperature in darkness.

Confocal microscopy, FRET and in vivo *imaging of organelles*

All microscopic observations were performed using a Zeiss LSM 510 laser confocal scanning microscope (LCSM: LSM510/ConfoCor2, Carl-Zeiss, Jena, Germany). H_2DCFDA, FDA, GFP, and Rh123 signals were visualized with excitation at 488 nm and emission at 500–550 nm using a band pass filter, and chloroplast autofluorescence (488 nm excitation) was visualized at 650 nm with a long pass filter. MitoTracker Red CMXRos signals were visualized in another detection channel using a 543 nm excitation light from a He-Ne laser and a 565–615 nm band pass filter. MitoSOX Red signals were visualized using a 510 nm excitation light and a 565–615 nm band pass filter. For FRET detection, the 458 nm laser line from an argon ion laser was attenuated with an acousto-optical tunable filter (AOTF), reflected by a dichroic mirror (main beam splitter HFT 458 nm), and focused through a Zeiss Plan-Neofluar ×40 (numerical aperture=1.3) oil-immersion objective lens onto the sample. Images were acquired through three channels. Two band-pass (BP) filters (BP 465–510 nm and BP 520–550 nm) were used for ECFP (ECFP channel) and EYFP (FRET channel), respectively, and the chlorophyll autofluorescence was collected with a 650–700 nm BP filter. All of the quantitative analysis of the fluorescence images was performed using Zeiss Rel4.2 image-processing software. Quantitative FRET analysis was carried out with correction (as described in Supplementary Fig. S1 at *JXB* online).

Live imaging of ROS and MTP

After Al treatment, the protoplasts were incubated with 5 μM H_2DCFDA in the presence or absence of 100 nM MitoTracker Red CMXRos for 30 min and then observed under LCSM. After Al treatment, the protoplasts were double-stained with Rh123 (2 μg ml^{-1}) and MitoTracker Red CMXRos (100 nM) for 30 min. The uptakes of Rh123 and MitoTracker into cells and into mitochondria were observed under LCSM.

Detection of mitochondrial ROS

After incubation with 5 μM H_2DCFDA or 5 μM MitoSOX Red for 30 min, isolated mitochondria (0.5 mg ml^{-1}) were treated with Al and the fluorescence intensity was measured with an LS 55 Luminescence Spectrophotometer (PerkinElmer, LS55, UK) at room temperature. The values at 525 nm or 580 nm were used to determine the fluorescence intensity of H_2DCFDA or MitoSOX Red, respectively.

Ultrastructural analysis

Arabidopsis mesophyll protoplasts were fixed and embedded as described previously (Yao *et al.*, 2001, 2004). For each treatment, at least three replicates were fixed and three sections from each replicate were analysed. The figures show representative images. For the observation of mitochondrial morphology, the samples were photographed under a transmission electron microscope (TEM, Philips CM-120, FEI Company, USA) at an accelerating voltage of 120 kV.

Measurement of mitochondrial membrane permeability

Isolated mitochondria treated with Al were suspended with 0.2% (w/v) BSA, and the concentration of mitochondrial proteins was adjusted to approximately 0.5 mg ml^{-1}. For mitochondrial membrane permeability detection, the absorbance at 540 nm was determined with a UV spectrophotometer (Zhang and Xing, 2008).

Protein extraction and caspase activity assays

Protoplasts (2×10^5 protoplast ml^{-1}) were placed on 24 well plates and incubated with 500 μM Al. At the indicated time points, protoplasts were harvested and kept at –80 °C. For protein extraction, treated protoplasts were resuspended in lysis buffer (50 mM TRIS-HCl, pH 8.0, 15 mM NaCl, 1% Triton X-100, and 100 mg ml^{-1}, phenylmethylsulphonyl fluoride) and incubated on ice with gentle shaking on a level shaker for 30 min. Samples were centrifuged for 5 min at 12 000 *g* and 4 °C, and the supernatants were transferred to new 1.5 ml tubes. Protein concentrations were determined by the method of Bradford. Caspase-3-like activity was measured by determining the cleavage of the fluorogenic caspase-3-like substrate Ac-DEVD-pNA using supernatant prepared from cell lysates. The extent of Ac-DEVD-pNA cleavage was measured as the change in A_{405} because of the release of free fluorescent pNA.

Total RNA extraction and semi-quantitative RT-PCR

Total RNA was extracted from Al-treated mesophyll protoplasts (2×10^5 protoplast ml^{-1}) of 3-week-old *Arabidopsis* according to the manufacturer's instructions using the TRI reagent (Sigma). The concentration of RNA was determined by measuring the optical density (OD) at 260 nm. First-strand cDNA was synthesized with the SuperScript II First-Strand Synthesis System for RT-PCR (Invitrogen). PCR was performed using the following primers. AOX1a: left, ATGATGATAACTCGCGGTGGAGC; right, GCAACATTCAAAGAAAGCCGAATC. ACTIN: left, TCGTGGTCCTTCTGCT; right, GCTTTTTAAGCCTTTGATCTTGAGAG.

Protoplast viability assay

After the indicated treatment and time point, protoplasts were incubated with 50 μM FDA for 5 min at room temperature in darkness to determine cell viability. The fluorescence of FDA was observed under the Zeiss LSM 510. Approximately 100 cells were measured for each treatment.

Statistical analysis

All assays were repeated independently for a minimum of three times. Data are represented as mean ±SD. Statistical analysis was performed with the Student's paired *t* test. Differences were considered statistically significant at * P <0.05, ** P <0.01.

Results

Effects of AsA and CsA on protoplast viability under Al stress

Given our previous results that about half of the protoplasts would be stained by FDA at 1 h after a 0.5 mM Al treatment (see Supplementary Fig. S2 at *JXB* online), this dose of Al (0.5 mM) was used to treat protoplasts in this work. To establish the mechanism of Al-induced protoplast death further, the effects of AsA, a natural antioxidant, and CsA, an inhibitor of MPTP opening, on protoplast survival were examined using FDA staining. The viable protoplasts were yellow for both red (chloroplast autofluorescence) and green-yellow (FDA); non-viable protoplasts were red for chloroplast autofluorescence only. As shown in Fig. 1, protoplasts preincubated with AsA or CsA exhibited an apparent increase in protoplast viability compared with protoplasts without pretreatments under Al stress (Fig. 1A). Quantitative analysis also showed that, at 60 min after the addition of Al, nearly 82±5% (P >0.05) and 78±9% (P >0.05) protoplast survival could be observed for protoplasts preincubated with AsA or CsA, respectively, whereas protoplast survival was only 50±6% (P <0.05) in the absence of AsA or CsA pretreatments (Fig. 1B). This result demonstrated that ROS and mitochondria dysfunction played vital roles in Al-induced protoplast death.

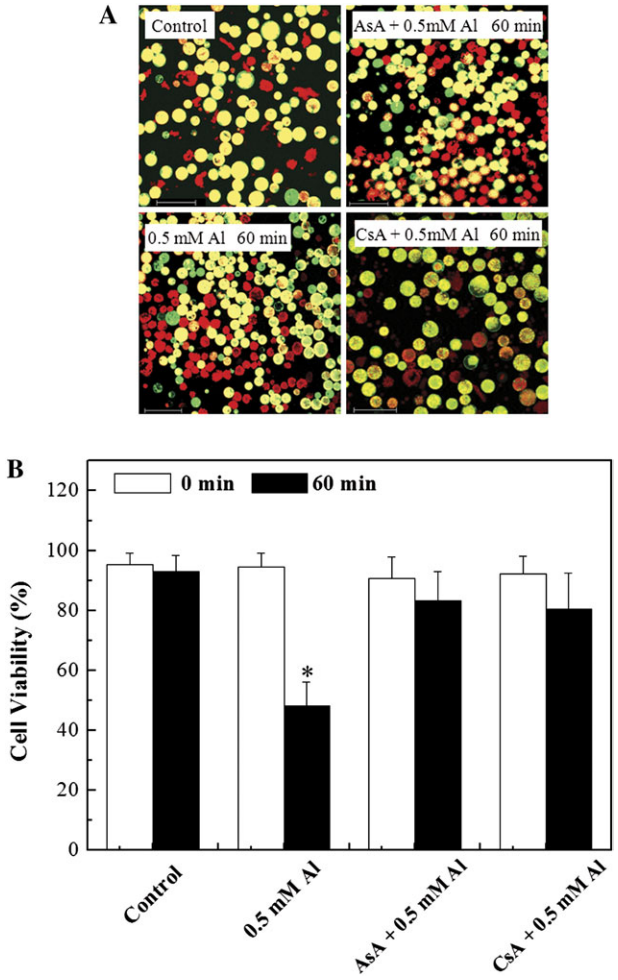

Fig. 1. Effects of AsA and CsA on Al-induced protoplast death. After 0.5 mM Al treatment, protoplasts (2×10^5 ml^{-1}) preincubated with 1 mM AsA or 50 μM CsA were incubated with 50 μM FDA and observed with a LCSM (A). The viable protoplasts were counted at the indicated times after Al treatments (B). Error bars are ±SD values for five replicates. Asterisks (*) indicate a significant difference from the Control at * P <0.05 by *t* test. Scale bars, 100 μm.

Al-induced mitochondrial ROS generation

Generation of ROS, such as hydrogen peroxide (H_2O_2) and superoxide, occurs in different cellular compartments and plays crucial roles in the stress response (Apel and Hirt, 2004). First, H_2O_2 production in Al-treated protoplasts was investigated using H_2DCFDA staining. H_2DCFDA is a non-fluorescent compound that can readily enter cells. Once inside cells, the acetate is cleaved by endogenous esterases. The acetate-free, reduced form of H_2DCF is trapped inside the cells and can be oxidized by H_2O_2 to form DCF, a highly fluorescent compound (Gao *et al.*, 2008). Flow cytometry analysis showed that, as early as 10 min after Al treatment, about 37.62% of protoplasts exhibited high DCF fluorescence compared with 5.63% of the control sample, and the amount of protoplasts with high DCF fluorescence was up to about 88.29% at 60 min after the Al treatment (see Supplementary Fig. S3 at *JXB* online). Supplementary Table S1 (at *JXB* online) summarized H_2O_2 production in three independent experiments. To confirm that the increased DCF fluorescence after Al treatment originated from mitochondria, protoplasts were coloaded with MitoTracker Red CMXRos, a cell-permeant dye that contained a mildly thiol-reactive chloromethyl moiety for labelling mitochondria. The data showed that protoplasts double-stained with DCF and MitoTracker Red CMXRos showed obvious fluorescent overlap that colocalized in the cytoplasmic areas in which mitochondria were present (Fig. 2A). To clarify the results quantitatively, the kinetics of H_2O_2 production was monitored in isolated mitochondria (Fig. 2B). At about 10 min after Al treatment, DCF fluorescence intensity began to increase and was obviously boosted at 20 min. Henceforth, the H_2O_2 level kept a slight increase until 60 min.

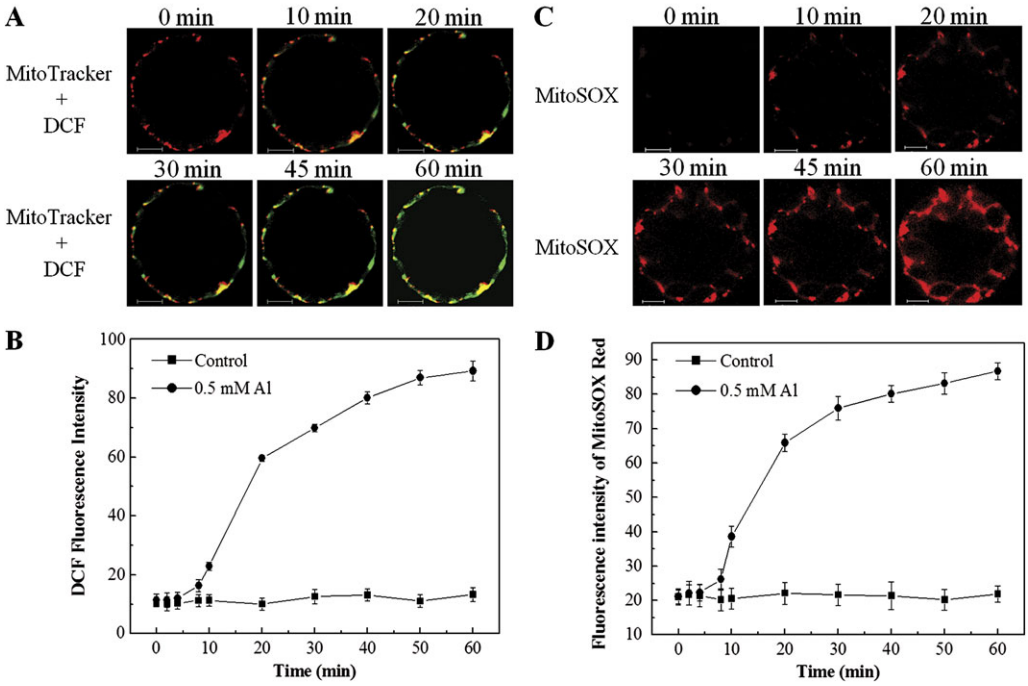

Fig. 2. Generation of mitochondrial ROS under Al stress. (A) The overlaid fluorescence imaging of DCF and MitoTracker Red CMXRos in *Arabidopsis* protoplasts. (B) Kinetics graphs of DCF signal intensity of Al-treated isolated mitochondria. (C) The fluorescence imaging of MitoSOX Red in *Arabidopsis* protoplasts. (D) Kinetics graphs of MitoSOX Red signal intensity of Al-treated isolated mitochondria. Scale bars, 10 μm. Error bars are ±SD values for three replicates.

Subsequently, the production of mitochondrial superoxide was measured using MitoSOX-Red staining. MitoSOX Red, a fluorogenic dye for the highly selective detection of mitochondrial superoxide in live cells, can be oxidized by superoxide and exhibits red fluorescence once in the mitochondria. Data showed that MitoSOX Red fluorescence began to emerge at 10 min after Al treatment, and was obviously boosted up at 20 min (Fig. 2C, D), which is consistent with the kinetics of mitochondrial H_2O_2 production. Taken together, the results indicated that H_2O_2 and superoxide formed from mitochondria are involved in an oxidative burst induced by Al.

Al-induced disturbance of mitochondrial morphology

As described above, ROS production induced by Al occurred in mitochondria (Fig. 2). Also, the mitochondria may be important targets for ROS, causing mitochondrial dysfunction. Thus, alterations in mitochondrial position or shape, one of the indicators of mitochondrial activity, were monitored during Al treatment (Fig. 3). To visualize the mitochondrial dynamics, protoplasts isolated from transgenic plants possessing mito-targeted GFP (S65T) were used. In control protoplasts, the majority of mitochondria appeared as typical elongated rods or filamentous structures and were evenly distributed in the cytoplasm. However, after Al treatment, most of the mitochondria had undergone morphological transition with the prolonged exposure to Al. The mitochondria first became swollen and spherical in shape (20 min), then irregularly clumped or clustered (40 min), and finally aggregated to be fused (60 min) within the cytoplasm, which could be alleviated by the addition of AsA to eliminate ROS (Fig. 3A). These results obtained by living imaging technique were supported by ultrastructural analysis (Fig. 3C). According to a previous study, mitochondrial swelling can also be detected as a rapid absorbance loss at 540 nm (Zhang and Xing, 2008). Our result showed that treating isolated mitochondria with 0.5 mM Al led to a progressive decline in their absorbance at 540 nm (Fig. 3B). At 60 min after Al treatment, the absorbance at 540 nm decreased to 36.9±6% (P <0.05) of the control sample, and pretreatment with AsA effectively delayed and inhibited the absorbance decrease (P >0.05).

Al-induced MTP loss

As another indicator of mitochondrial activity, the changes in MTP induced by Al were examined using Rh123, a specific fluorescent probe to monitor active mitochondria. The mitochondria-specific marker MitoTracker Red CMXRos was also used to confirm that Rh123 was mainly localized to mitochondria. Under Al treatment, the protoplasts showed a time-dependent decrease in MTP compared with the control protoplasts (Fig. 4B). Under LCSM, the control protoplasts were stained extensively with Rh123, the fluorescence of which co-localized with MitoTracker, thus establishing the specificity of Rh123 for mitochondria (Fig. 4A). After treatment with 0.5 mM Al for 20 min, the fluorescence intensity of Rh123 began to decrease; a further decrease was observed at 60–80 min (Fig. 4B). At 60 min,

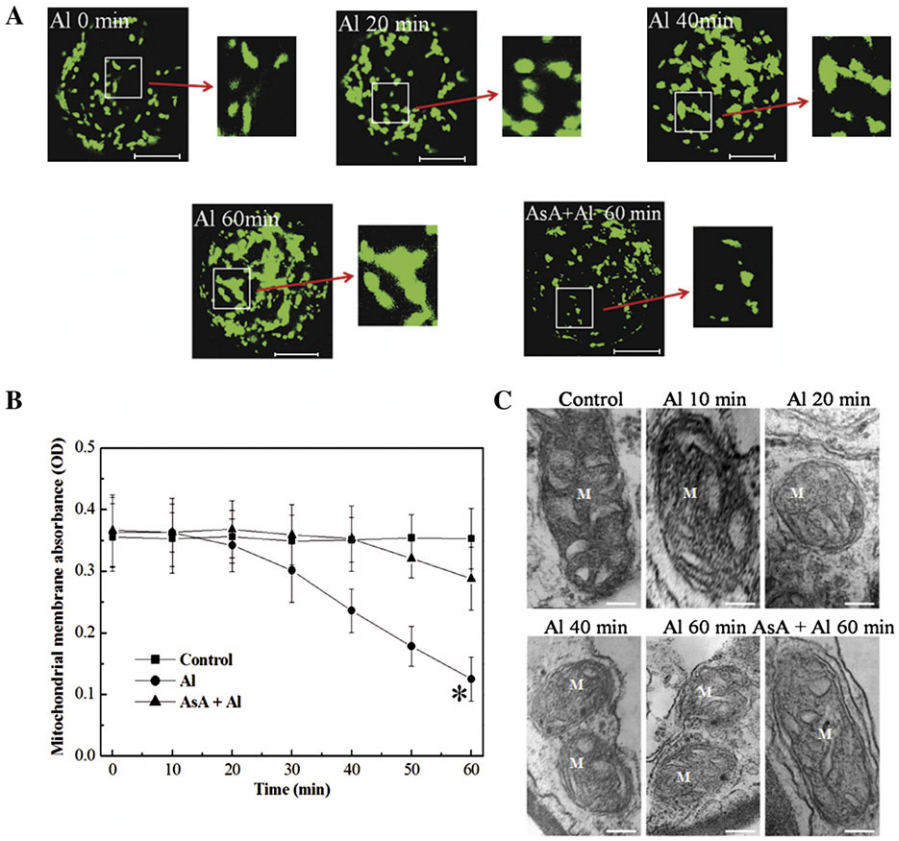

Fig. 3. Transition of mitochondrial morphology and swelling of isolated mitochondria during Al treatment. (A) 3D reconstructed images of mito-GFP-expressing mesophyll protoplasts treated with 0.5 mM Al with or without pretreatment of 1 mM AsA. Scale bars=10 μm. (B) Mitochondrial swelling indicated by the changes in absorbance at 540 nm. Error bars are ±SD values for five replicates. Asterisks (*) indicate a significant difference from the Control at * P <0.05 by t test. (C) Ultrastructural analysis of mitochondrial morphology transition. Mesophyll protoplasts treated with 0.5 mM Al with or without pretreatment of 1 mM AsA were observed with TEM. M, mitochondria. Scale bars, 200 nm.

only the clusters of mitochondria could be stained with Rh123 and MitoTracker. At 80 min, the protoplasts were stained at very low intensity or even not stained (Fig. 4A, B). The protoplasts preincubated with AsA before Al treatment could be stained with Rh123 compared with those without AsA at 80 min after Al treatment (Fig. 4). To confirm the single-cell experiment, a flow cytometry analysis was carried out (see Supplementary Fig. S4 at *JXB* online). Al treatment of protoplasts induced a rapid and progressive loss of MTP detectable as early as 30 min after incubation (see Supplementary Fig. S4D at *JXB* online). At this time, Al-treated protoplasts showed over 80% viability (see Supplementary Fig. S2 at *JXB* online), indicating that MTP breakdown was an early event during Al-induced PCD. Subsequently, the percentage of protoplasts exhibiting a high MTP decreased further to 33.37% at 60 min of Al incubation (see Supplementary Fig. S4E at *JXB* online), and 8.79% after 80 min (see Supplementary Fig. S4F at *JXB* online). However, about 85.19% of protoplasts pretreated with AsA still exhibited a high MTP at 60 min after Al treatment (see Supplementary Fig. S4G at *JXB* online). Supplementary Table S2 (at *JXB* online) summarized MTP changes in three independent experiments.

Activation of caspase-3-like protease induced by Al

FRET imaging was used to detect the *in vivo* caspase-3-like protease activation in transfected protoplasts with the fusion protein ECFP-DEVD-EYFP. After Al exposure for 30 min, the EYFP/ECFP FRET in the transfected protoplasts decreased with the decreasing EYFP fluorescence intensity (Fig. 5C, D) when compared with those without Al exposure (Fig. 5A, B), suggesting the occurrence of the cleavage of the fusion protein ECFP-DEVD-EYFP. The temporal profile of EYFP/ECFP emission ratio measured in a single cell showed that, after 0.5 mM Al exposure, the EYFP/ECFP ratio remained almost unchanged within the first 30 min, then it started to decrease gradually and reached a minimum at 100 min (Fig. 5D), indicating that the caspase-3-like protease was activated and the fusion protein ECFP-DEVD-EYFP was cleaved in a time-dependent manner in the transfected protoplasts after Al treatment. It should be noted that, during the whole investigation period, the protoplast morphology remained intact (Fig. 5; DIC images); therefore, the decrease of EYFP fluorescence and FRET ratio should be due to the caspase-3-like protease activation and the subsequent cleavage of ECFP-DEVD-EYFP during Al-induced PCD, not to the rupture of

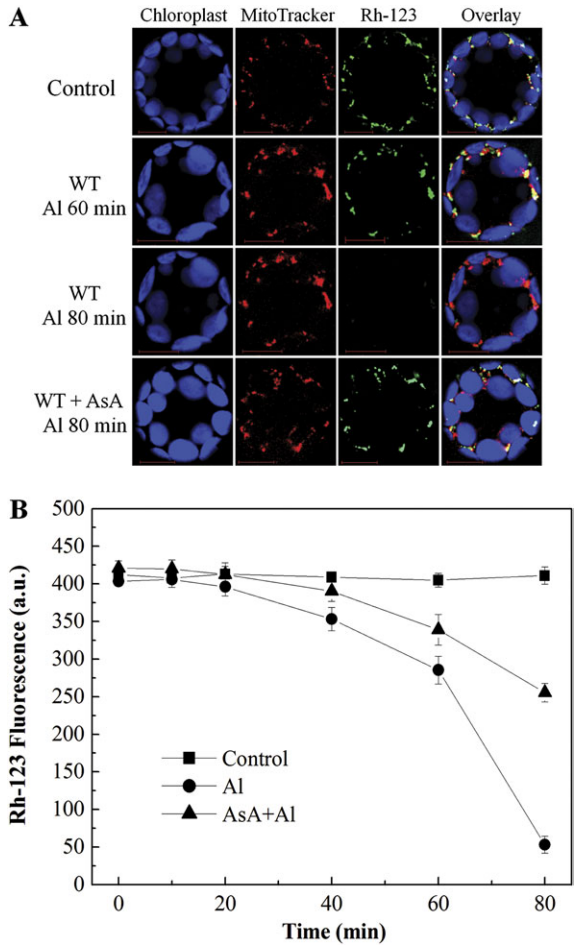

Fig. 4. Disruption of the MTP after Al treatment. (A) Images of Rh123 fluorescence in Al-treated mesophyll protoplasts in the presence or absence of 1 mM AsA. (B) Curve of fluorescence intensity of Rh123 in protoplasts treated with 0.5 mM Al with or without pretreatment of 1 mM AsA. Scale bars, 10 μm. Error bars are ±SD values for three replicates.

protoplasts. By contrast, in the transfected protoplasts without Al treatment, the EYFP fluorescence and the EYFP/ECFP FRET ratio underwent only a slight decrease during the whole investigation period (Fig. 5A, B), indicating that there was no change in FRET during the process. Subsequently, the caspase-3-like activity was measured in protoplast extracts using the caspase-3 fluorogenic substrate Ac-DEVD-pNA. The results demonstrated that the induction of caspase-3-like activity was detected in the protoplasts at 30 min after Al treatment, reached a peak at 80 min, and subsequently decreased with the increase of the treatment time of Al (Fig. 6).

CsA delayed mitochondrial dysfunction and caspase-3-like activation under Al stress

As described above, Al stress induced MTP decrease (Fig. 4; see Supplementary Fig. S4 at JXB online). The results of flow cytometry analysis showed that pretreatment with CsA effectively inhibited the decrease of Rh123 fluorescence intensity and 90.57% of protoplasts maintained high Rh123 fluorescence at 60 min after Al treatment, in contrast to 33.37% of protoplasts unpretreated with CsA (see Supplementary Fig. S4E, H at *JXB* online). Furthermore, the effect of CsA on caspase-3-like activation was investigated. After being pretreated with CsA, the caspase-3-like activation was delayed to about 55 min after Al exposure, compared with the protoplasts without CsA pretreatment in which the caspase-3-like activation occurred at 30 min after Al exposure (Figs 5E, F, 6). These results indicated that Al induction of mitochondria MTP loss and caspase-3-like activation was dependent on the opening of MPTP.

Changes of respiratory complex activities and Fe–S protein contents under Al treatment

As the important sources and subcellular sites of mitochondrial ROS generation under adverse stresses, the activities of complex I and III in mitochondrial electron transport chains were determined under Al treatment. Results showed that both complex I and III activities exhibited a time- and concentration-dependent decrease (Fig. 7A, B). As early as 5 min after 0.5 mM Al treatment, the activities of complex I and III obviously began to decrease, which is prior to mitochondrial ROS production (Fig. 2). Moreover, pretreatment with 1 mM AsA failed to inhibit the decline in the activities of both complex I and III (Fig. 7C, D), indicating that complex I and III as the targets of Al phytotoxicity might be directly damaged by Al instead of in a ROS-dependent manner. Subsequently, the content of Iron–Sulphur (Fe–S) protein, an important component of complex I and III in the mitochondrial respiratory chains, was measured using its specific absorbance in 400 nm (Roland and Ulrich, 2006). Our results showed that the Fe–S protein content also exhibited a time- and concentration-dependent decrease (Fig. 7E). After 0.5 mM Al treatment, an immediate decline (within 100 s) in 400 nm absorbance was noted, and in about 10 min the A_{400} value was decreased to a very low level, which was also not inhibited by the addition of AsA (Fig. 7F). These results suggest the possible mechanism of mitochondrial ROS production: that Al might directly interact with the Fe–S protein to cause damage to complex I and complex III, resulting in the disruption of electron transfer chains and a subsequent oxidative burst.

AOX1a alleviated Al-induced protoplast death

AOX1a is often dramatically induced at the transcript level by a variety of stresses (Millenaar and Lambers, 2003). The RT-PCR assay showed that the *AOX1a* gene was expressed at a basal level in the control condition, and its transcript level increased during Al stress in a time-dependent manner (Fig. 8A). At 15 min after 0.5 mM Al treatment, a significant difference at $P < 0.05$ in the expression level of *AOX1a* was observed relative to the untreated control samples. At 30 min and 60 min after Al treatment, the increase in *AOX1a* expression was up to 3.5-fold ($P < 0.01$) and 4.5-fold

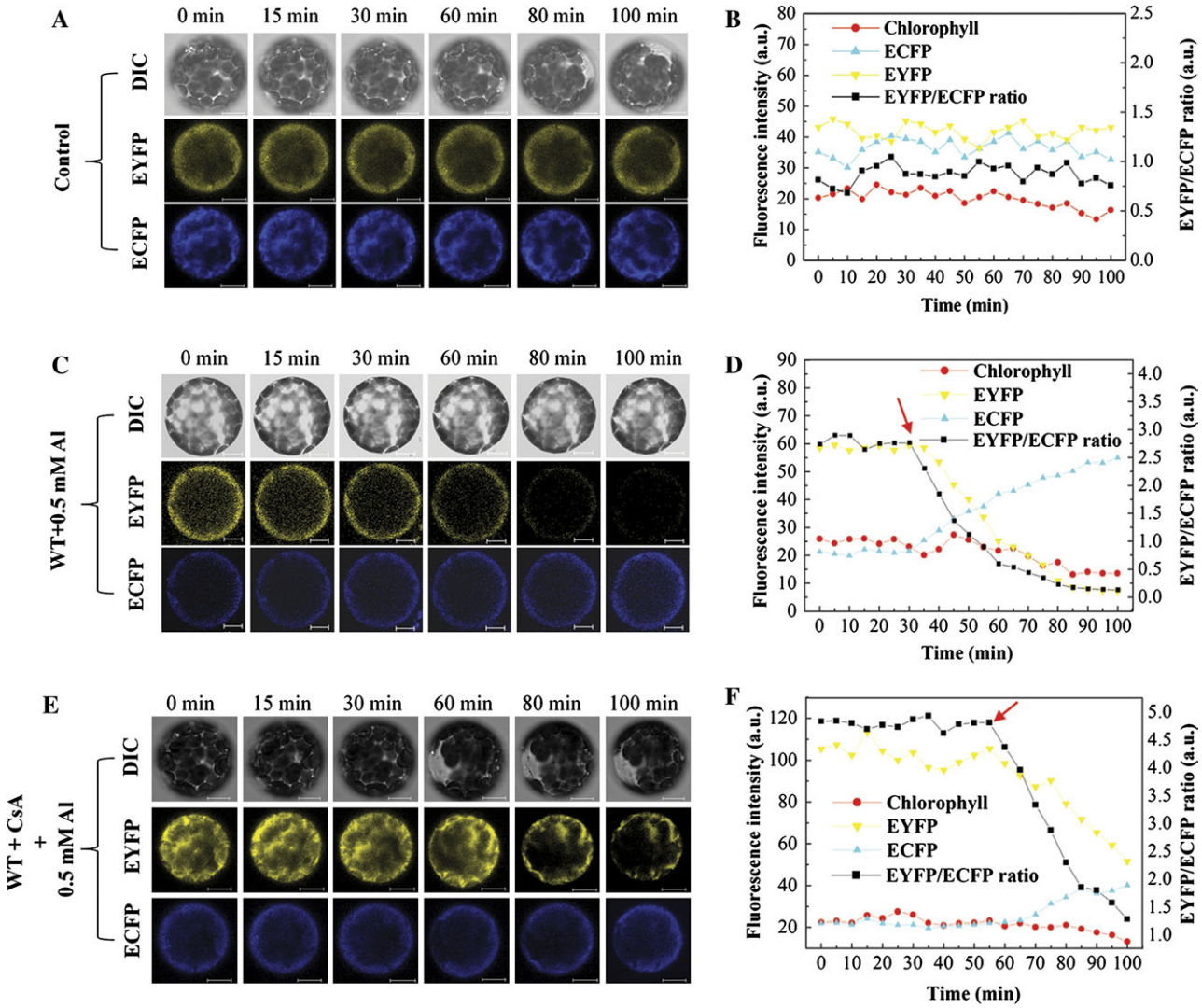

Fig. 5. Dynamics of caspase-3-like activation in response to Al treatment. (A, B, C, D) The transfected protoplasts without (A, B) or with (C, D) Al treatment were excited by a 458 nm laser. (E, F) After pretreatment with 50 μM CsA, the transfected protoplasts treated with 0.5 mM Al were excited by a 458 nm laser. ECFP, EYFP, and EYFP/ECFP FRET images were recorded, and the fluorescence intensity of ECFP, EYFP, and chlorophyll as well as the EYFP/ECFP ratio were measured during a time lapse. The arrows indicate the start of the decrease of EYFP/ECFP ratio. Representative images and data from one experiment are presented. Repetition of experiments led to results very similar to those shown. a.u., Arbitrary units; DIC, differential interference contrast. Bars, 10 μm.

(P <0.01) of the control level, respectively (Fig. 8B). Subsequently, the role of AOX1a in Al-induced protoplast death was investigated (Fig. 8C, D). Results showed that protoplasts lacking the *AOX1a* gene (aox1a) exhibited much lower protoplast viability (23±4%, P <0.01) than WT protoplasts (48±9%, P <0.05) at 60 min after Al treatment. However, in the protoplasts over-expressing the *AOX1a* gene (AOX1a-OE), protoplast viability at 60 min after Al treatment was up to 87±9% (P >0.05).

Discussion

This study is an attempt to understand the mitochondria-dependent mechanism of PCD induced by Al phytotoxicity, through the investigation of a cascade of phenomena in Al-exposed *Arabidopsis* protoplasts using fluorescence techniques.

In the study of apoptotic mechanisms, ROS have been recognized as crucial players both in animal and plant cells (Simon *et al.*, 2000; Van Breusegem and Dat, 2006). Mitochondria, as the common organelle in animals and plants, have received considerable attention in the investigation of ROS-dependent PCD. Intracellular ROS generated from the mitochondrial electron transport chain can directly interact with mitochondrial proteins and lipids, causing their dysfunction (Yao *et al.*, 2002; Chen *et al.*, 2003; Hiroko *et al.*, 2007). Lipid peroxidation prompts the release of mitochondrial cytochrome *c* into the cytosol and

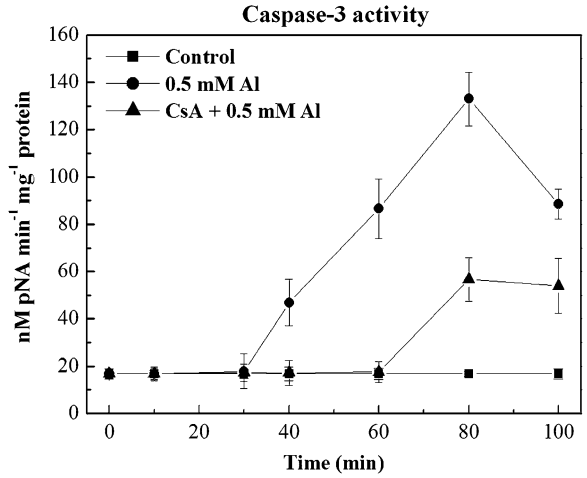

Fig. 6. Caspase-3-like activity tested in an *in vitro* assay using the caspase-3 substrate. The extracts from protoplasts treated with 0.5 mM Al at the indicated times were used. The samples were incubated with the caspase-3 substrate Ac-DEVD-pNA (200 mM) in assay buffer containing phenylmethylsulphonyl fluoride and EDTA. Error bars indicate SD values for five replicates.

the permeabilization of mitochondrial outer membrane (Jeffrey, 2006; Orrenius *et al.*, 2007). Taken together, mitochondria play crucial roles in ROS-dependent PCD (Simon *et al.*, 2000; Yao *et al.*, 2002; Noctor *et al.*, 2006; Hiroko *et al.*, 2007; Mayank *et al.*, 2007). In our experiments, a quick burst of ROS formation occurred in Al-treated protoplasts, and the ROS generated from mitochondria were demonstrated to be involved in the oxidative burst induced by Al (Fig. 2; see Supplementary Fig. S3 at *JXB* online).

The mitochondrial electron transport system generates oxygen radicals through electron leaks as substrates are metabolized. Complex I and III of the electron transport chain are recognized as the major sites for ROS production (Castello *et al.*, 2007; Murphy, 2009). Previous studies with metal cations in potato, corn, and pea mitochondria have showed respiratory inhibitions (Bittell *et al.*, 1974; Kesseler and Brand, 1995; Dixit *et al.*, 2002). In animal mitochondria, treatment with Pb, Cd, Zn, and Hg cause the inhibition of complex III activity (Kleiner, 1974). Inhibition of electron flow and respiration rate has been shown under Al treatment (Yamaguchi *et al.*, 1999; Yamamoto *et al.*, 2002); however, how Al ion affects mitochondrial functions has not yet been elucidated. As previously described (Panda *et al.*, 2008), it is possible that Al may inhibit mitochondrial respiration through its binding and interaction to functional proteins and metal ions (Fe or Cu) in the electron carriers of the mitochondria electron transport chain. Our results showed that complex I and III activities were affected by Al in a time- and concentration-dependent manner, which could not be alleviated by eliminating ROS, indicating that Al might act directly on these complexes (Fig. 7). Fe–S proteins are impotent cofactors of complex I and III in the mitochondrial electron transport chains, and play crucial roles in the electron transport system. The simplest form of an Fe–S centre is the rhombic [2Fe–2S] cluster. In some of these complex Fe–S proteins, other metals such as molybdenum, vanadium or nickel may replace one of the Fe ions or may be present in addition to the Fe ions (Roland *et al.*, 2006; Roland and Ulrich, 2006; Giuseppe *et al.*, 2009). Al and Fe ions have high similarity in their chemical characters, and in some cases Al can replace Fe in Fe-containing proteins and Fe transporters (Fleming and Joshi, 1987; Cannata-Andia, 1996). Our data showed a ROS-independent decrease of Fe–S protein content under Al treatment (Fig. 7E, F), indicating that Al might directly destroy the structure or halt the synthesis and assembly of Fe–S proteins. In all, it was supposed that Al, possibly through its direct interaction with Fe–S proteins, caused complex I and III damage, resulting in the subsequent mitochondrial oxidative burst.

AOX, as the unique respiratory terminal oxidase in plants, plays important roles to protect respiratory electron transport and alleviate a mitochondrial oxidative burst under stress. AOX1a is often dramatically induced at the transcript level by a variety of stresses (Millenaar and Lambers, 2003; Plaxton and Podesta, 2006). Our data showed that the expression of the *AOX1a* gene was up-regulated by Al stress, and over-expression of *AOX1a* in protoplasts resulted in enhanced Al tolerance (Fig. 8), indicating the protective roles of *AOX1a* against Al toxicity.

In animal cells, the significance of MPT during apoptosis has been well documented (Kroemer, 1999; Jeffrey, 2006). During UV-induced mammalian cell apoptosis the MTP loss occurs accompanied by the activation of Bid, a Bcl2 interacting protein that can mediate the release of cytochrome *c* from mitochondria in response to the activation of a cell surface death receptor (Wu *et al.*, 2007). In plant cells, the ROS-dependent collapse of MTP is also indispensable for the execution of stress-induced PCD (Yao *et al.*, 2004; Hauser *et al.*, 2006). As another indicator of mitochondrial activity, mitochondrial localization and morphology have been related to physiological function and energy metabolism of the organelle (Logan, 2006). It has been reported that ROS stress can elicit the morphological disruption of mitochondria under various stimuli (Gao *et al.*, 2008; Zhang and Xing, 2008). Here, our results showed that the mitochondrial swelling and decrease in MTP occurred before cell death in the early stages of Al-induced PCD. The antioxidant molecule, AsA, could effectively alleviate Al-induced mitochondrial swelling and MTP loss (Figs 3, 4; see Supplementary Fig. 4 at *JXB* online), and partially decreased the percentage of protoplasts undergoing PCD (Fig. 1). Our data demonstrated that ROS acted as signalling molecules in Al-induced protoplast PCD, and the ROS-dependent mitochondrial dysfunction was an early event in this process.

In many animal cell apoptosis pathways, the crucial and final step is believed to be caspase activation. Several studies have suggested that the executions of plant PCD also

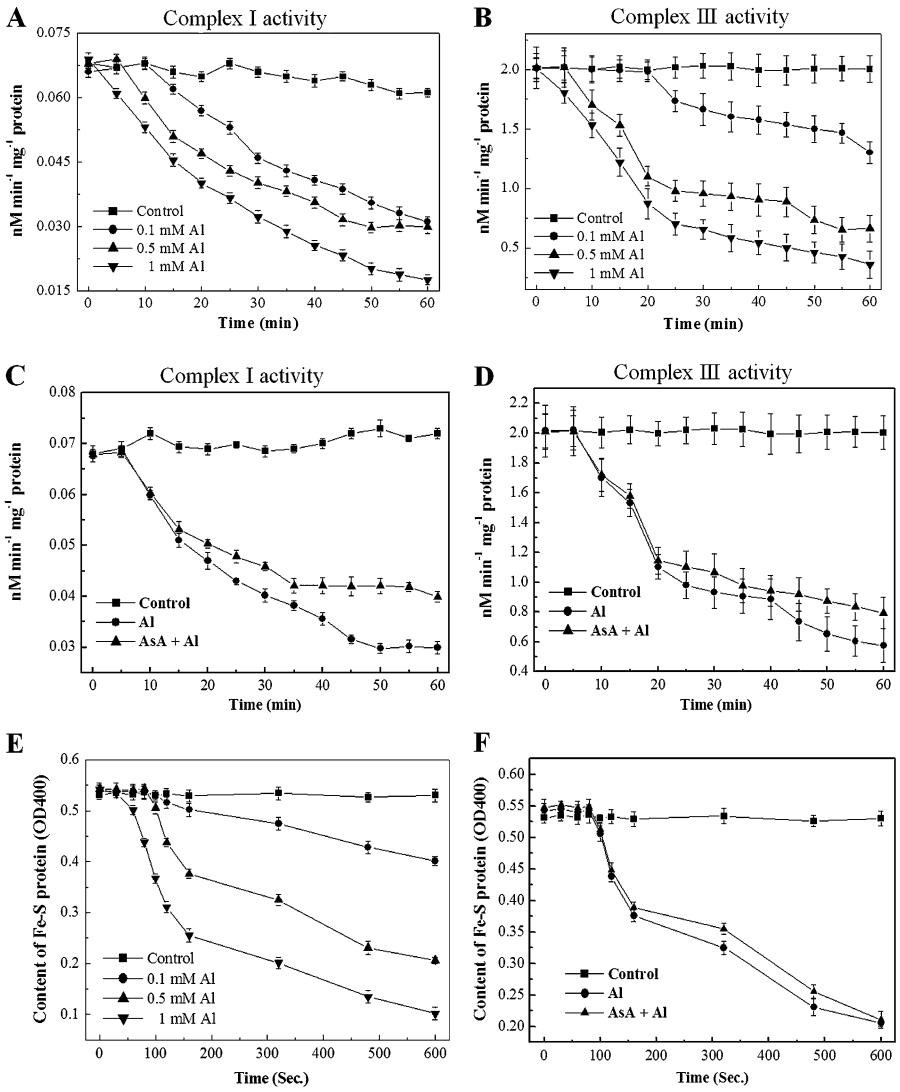

Fig. 7. Changes of respiratory complexes activity and content of Fe–S protein after Al treatment and the effect of AsA on the activity of the complexes and Fe–S content. (A, B, C, D) The activities of complex I and III in Al-treated isolated mitochondria without (A, B) or with (C, D) pretreatment of 1 mM AsA. (E, F) Measurement of Fe–S protein content in Al-treated isolated mitochondria without (E) or with (F) pretreatment of 1 mM AsA using the change in A_{400}. Error bars are ±SD values for five replicates.

require the activation of caspase-like activity (del Pozo and Lam, 1998; Mlejnek and Prochazka, 2002). Among various kinds of caspases, caspase-3, which can induce DNA fragmentation and chromatin condensation, is considered to be the major executioner in the PCD of animal cells. In this work, the Al-induced caspase-3-like activation was detected using a FRET probe which has been successfully used to monitor UV-induced caspase-3-like activation in *Arabidopsis* protoplasts (Zhang *et al.*, 2009). Furthermore, pretreatment with CsA, an inhibitor of MPTP, retarded the mitochondrial dysfunction and further caspase-3-like activation (Figs 5, 6). These results suggested that mitochondrial MTP loss played an important role in the regulation of plant PCD induced by Al stress.

According to our experimental results, a potential cascade of cellular events during Al-induced PCD was proposed following a temporal sequence (Fig. 9): Al, after entering mitochondria, interacted with Fe–S protein of complex I and III, and inhibited the activity of the electron transport chain, resulting in the excess electron and massive production of mitochondrial ROS. Subsequently, the generation of ROS directly or possibly through mediating other processes, induced MPT, thus promoted mitochondria inner membrane permeabilization and caused the swelling of mitochondria, the rupture of the mitochondrial outer membrane, and then the release of cytochrome *c*, which, in turn, activated caspase-3-like pathway and finally resulted in PCD.

In conclusion, our data showed that the mitochondrial ROS generation, decrease of MTP, and the activation of caspase-3-like, in that order, played a crucial role in Al-induced *Arabidopsis* protoplast PCD. Our study contributed to the understanding of the mitochondria-dependent mechanism of the Al-induced biological responses in the

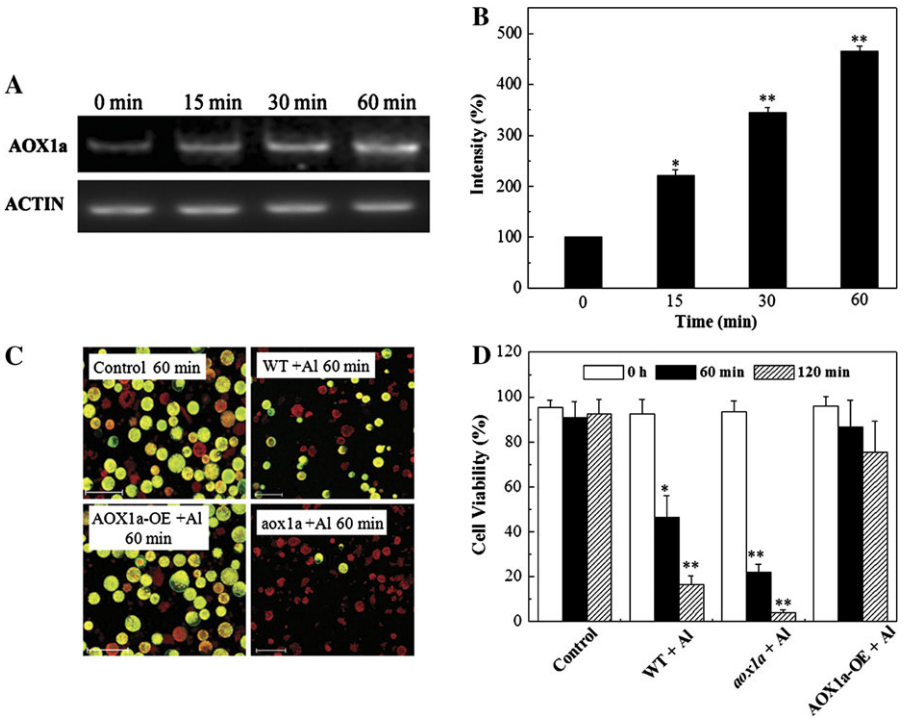

Fig. 8. Involvement of AOX1a in protoplast death induced by Al. (A) Representative analysis of AOX1a gene expression under Al treatment using RT-PCR. (B) Quantitative analysis of AOX1a gene expression shown in (A) with Image J software. Intensity of control was set as 100%. Data represent means ±SD of three independent experiments. (C, D) Effect of AOX1a on Al-induced protoplast death. After 0.5 mM Al treatment, protoplasts (2×10^5 ml^{-1}) from WT and transgenic *Arabidopsis* over-expressing (AOX1a-OE) or lacking (aox1a) the *AOX1a* gene were incubated with 50 μM FDA and observed with a LCSM. Error bars are ±SD values for five replicates. Asterisks (*) indicate a significant difference from the Control at * P <0.05 or ** P <0.01 by t test. Scale bars=100 μm.

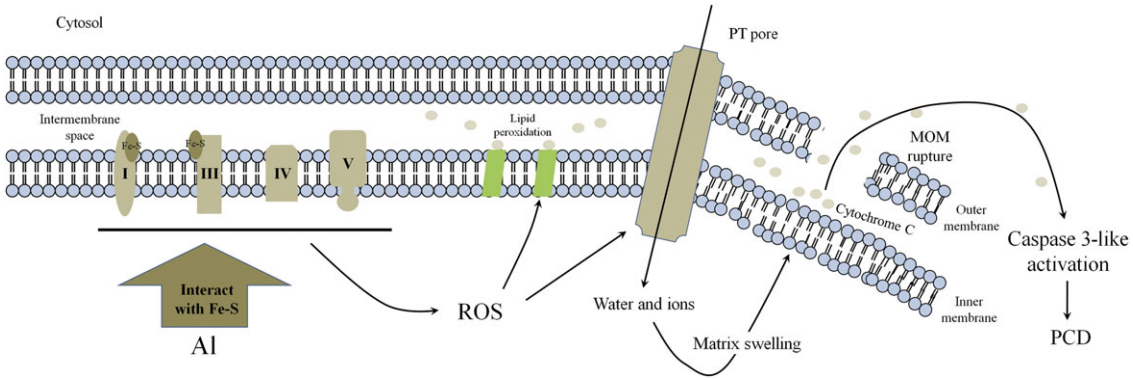

Fig. 9. Proposed working models for mitochondria-dependent PCD induced by Al. PT pore, permeabilization transition pore; MOM, mitochondria outer membrane; PCD, programmed cell death; Fe–S, iron–sulphur protein.

temporal sequence, and provided a new insight into the cellular signalling cascade of Al-induced plant PCD.

Supplementary data

Supplementary data can be found at *JXB* online.

Supplementary Fig. S1. Schematic representation and working principle of genetic reporter ECFP-DEVD-EYFP fusion proteins.

Supplementary Fig. S2. Concentration- and time-dependent protoplast death induced by Al.

Supplementary Fig. S3. Estimation of Al-induced changes of H_2O_2 by flow cytometry using H_2DCFDA.

Supplementary Fig. S4. Disruption of the MTP in Al-treated *Arabidopsis* protoplasts and effect of CsA or AsA on Al-induced MTP loss by flow cytometry using Rh123.

Supplementary Table S1. Flow cytometry analysis of H_2O_2 production in Al-treated protoplasts.

Supplementary Table S2. Flow cytometry analysis of MTP loss in Al-treated protoplasts.

Acknowledgements

We are grateful to Dr David C Logan (St Andrews, UK) for kindly providing transgenic *Arabidopsis* seeds harboring GFP-labelled mitochondria. This research is supported by the Programme for Changjiang Scholars and the Innovative Research Team in the University (IRT0829) and the National High Technology Research and Development Programme of China (863 Programme) (2007AA10Z204).

References

Apel K, Hirt H. 2004. Reactive oxygen species: metabolism, oxidative stress, and signal transduction. *Annual Review of Plant Biology* **55,** 373–399.

Bittell JE, Koeppe DE, Miller RJ. 1974. Sorption of heavy metal cations by corn mitochondria and the effects on electron and energy transfer reactions. *Physiologia Plantarum* **30,** 226–230.

Boscolo PRS, Menossi M, Jorge RA. 2003. Aluminium-induced oxidative stress in maize. *Phytochemistry* **62,** 181–189.

Cannata-Andia JB. 1996. Aluminium toxicity: its relationship with bone and iron metabolism. *Nephrology Dialysis Transplantation* **11,** 69–73.

Castello PR, Drechsel DA, Patel M. 2007. Mitochondria are a major source of paraquat-induced reactive oxygen species production in the brain. *Journal of Biological Chemistry* **282,** 14186–14193.

Chen Q, Vazquez EJ, Moghaddas S, Hoppel CL. 2003. Production of reactive oxygen species by mitochondria. *Journal of Biological Chemistry* **278,** 36027–36031.

Danon A, Delorme V, Mailhac N, Gallois P. 2000. Plant programmed cell death: a common way to die. *Plant Physiology and Biochemistry* **38,** 647–655.

del Pozo O, Lam E. 1998. Caspases and programmed cell death in the hypersensitive response of plants to pathogens. *Current Biology* **88,** 1129–1132.

Dixit V, Pandey V, Shyam R. 2002. Chromium ions inactivate electron transport and enhance superoxide generation *in vivo* in pea (*Pisum sativum* L. cv. Azad) root mitochondria. *Plant, Cell and Environment* **25,** 687–693.

Doyle SM, Diamond M, McCabe PF. 2010. Chloroplast and reactive oxygen species involvement in apoptotic-like programmed cell death in *Arabidopsis* suspension cultures. *Journal of Experimental Botany* **61,** 473–482.

Fleming J, Joshi JG. 1987. Ferritin: isolation of aluminium-ferritin complex from brain. *Proceedings of the National Academy of Sciences, USA* **84,** 7866–7870.

Fu HJ, Hu QS, Lin Z, Ren TL, Song H, Cai CK, Dong SZ. 2003. Aluminium-induced apoptosis in cultured cortical neurons and its effect on SAPK/JNK signal transduction pathway. *Brain Research* **980,** 11–23.

Gao CJ, Xing D, Li LL, Zhang LR. 2008. Implication of reactive oxygen species and mitochondrial dysfunction in the early stages of plant programmed cell death induced by ultraviolet-C overexposure. *Planta* **227,** 755–767.

Ghribi O, Herman MM, Spaulding NK, Savory J. 2002. Lithium inhibits aluminium-induced apoptosis in rabbit hippocampus, by preventing cytochrome *c* translocation, Bcl-2 decrease, Bax elevation, and caspase-3 activation. *Journal of Neurochemistry* **82,** 137–145.

Giuseppe C, Elisa F, Claudio L, Anna MR. 2009. Cadmium and mitochondria. *Mitochondrion* **9,** 377–384.

Hauser BA, Sun K, Oppenheimer DG, Sage TL. 2006. Changes in mitochondrial membrane potential and accumulation of reactive oxygen species precede ultrastructural changes during ovule abortion. *Planta* **223,** 492–499.

Hiroko PI, Mercy D, Hsiu-Chuan Y, Shigeaki S, Kazuo T, Takeshi N, Masahiro H, Yasutoshi K, Toshihiko O, Hideyuki JM. 2007. Evidence of ROS generation by mitochondria in cells with impaired electron transport chain and mitochondrial DNA damage. *Mitochondrion* **7,** 106–118.

Jeffrey SA. 2006. The role of the mitochondrial permeability transition in cell death. *Mitochondrion* **6,** 225–234.

Keith DR, Eric JS, Yogesh KS, Keith RD, Richard CG. 1998. Aluminium induces oxidative stress genes in. *Arabidopsis thaliana. Plant Physiology* **116,** 409–418.

Kesseler A, Brand MD. 1995. The mechanism of the stimulation of state 4 respiration by cadmium in potato tuber (*Solanum tuberosum*) mitochondria. *Plant Physiology and Biochemistry* **33,** 519–528.

Kleiner D. 1974. The effect of Zn^{2+}on mitochondrial electron transport. *Archives of Biochemistry and Biophysics* **165,** 121–125.

Kroemer G. 1999. Mitochondrial control of apoptosis: an overview. *Biochemical Society Symposia* **66,** 1–15.

Logan DC. 2006. Plant mitochondrial dynamics. *Biochimica et Biophysica Acta* **1763,** 430–441.

Logan DC, Leaver CJ. 2000. Mitochondria-targeted GFP highlights the heterogeneity of mitochondrial shape, size and movement within living plant cells. *Journal of Experimental Botany* **51,** 865–871.

Mayank S, Himani S, Neeta S. 2007. Hydrogen peroxide induces apoptosis in HeLa cells through mitochondrial pathway. *Mitochondrion* **7,** 367–373.

Millenaar FF, Lambers H. 2003. The alternative oxidase: *in vivo* regulation and function. *Plant Biology* **5,** 2–15.

Mlejnek P, Prochazka S. 2002. Activation of caspase-like proteases and induction of apoptosis by isopentenyladenosine in tobacco BY-2 cells. *Planta* **215,** 158–166.

Moller IM, Rasmusson AG. 2005. Isolation of mitochondria. In: Taiz L, Zeiger E, eds. *Plant Physiology*, 4th ed. Chapter 11.

Murphy MP. 2009. How mitochondria produce reactive oxygen species? *Biochemical Journal* **417,** 1–13.

Noctor G, Paepe RD, Foyer CH. 2006. Mitochondrial redox biology and homeostasis in plants. *Trends in Plant Science* **12,** 125–134.

Orrenius S, Gogvadze V, Zhivotovsky B. 2007. Mitochondrial oxidative stress: implications for cell death. *Annual Review of Pharmacology and Toxicology* **47,** 143–183.

Panda SK, Yamamoto Y, Kondo H, Matsumoto H. 2008. Mitochondrial alterations related to programmed cell death in tobacco

cells under aluminium stress. *Comptes Rendus Biologies* **311,** 597–610.

Plaxton WC, Podesta FE. 2006. The functional organization and control of plant respiration. *Critical Reviews in Plant Sciences* **25,** 159–198.

Roland L, Ulrich M. 2006. Iron–sulphur protein biogenesis in eukaryotes: components and mechanisms. *Annual Review of Cell and Developmental Biology* **22,** 457–486.

Roland L, Rafal D, Hans-Perter E, Anja H, Daili JAN, Antonio JP, Oliver S, Eugen U, Ulrich M. 2006. Mechanisms of iron–sulphur protein maturation in mitochondria, cytosol and nucleus of eukaryotes. *Biochimica et Biophysica Acta* **1763,** 652–667.

Simon HU, Haj-Yehia A, Levi-Schaffer F. 2000. Role of reactive oxygen species (ROS) in apoptosis induction. *Apoptosis* **5,** 415–418.

Vacca RA, Valenti D, Bobba A, Merafina RS, Passarella S, Marra E. 2006. Cytochrome *c* is released in a reactive oxygen species-dependent manner and is degraded via caspase-like proteases in tobacco Bright-Yellow 2 cells en route to heat shock-induced cell death. *Plant Physiology* **141,** 208–219.

Van Breusegem F, Dat JF. 2006. Reactive oxygen species in plant cell death. *Plant Physiology* **141,** 384–390.

Wagner D, Przybyla D, Opden Camp R, *et al*. 2004. The genetic basis of singlet oxygen-induced stress responses of Arabidopsis thaliana. *Science* **306,** 1183–1185.

Wang X. 2001. The expanding role of mitochondria in apoptosis. *Genes and Development* **15,** 2922–2933.

Wu YY, Xing D, Liu L, Chen TS, Chen WR. 2007. Fluorescence resonance energy transfer analysis of bid activation in living cells during ultraviolet-induced apoptosis. *Acta Biochimica et Biophysica Sinica* **39,** 37–45.

Yakimova ET, Kapchina-Toteva VM, Woltering EJ. 2007. Signal transduction events in aluminium-induced cell death in tomato suspension cells. *Journal of Plant Physiology* **164,** 702–708.

Yamamoto Y, Kobayashi Y, Rama DS, Sanae R, Matsumoto H. 2002. Aluminium toxicity is associated with mitochondrial dysfunction and the production of reactive oxygen species in plant cells. *Plant Physiology* **128,** 63–72.

Yamaguchi Y, Yamamoto Y, Matsumoto H. 1999. Cell death process initiated by a combination of aluminium and iron in suspension-cultured tobacco cells. *Soil Science and Plant Nutrient* **45,** 647–657.

Yao N, Bartholomew JE, James M, Greenberg JT. 2004. The mitochondrion: an organelle commonly involved in programmed cell death in Arabidopsis thaliana. *The Plant Journal* **40,** 596–610.

Yao N, Tada Y, Park P, Nakayashiki H, Tosa Y, Mayama S. 2001. Novel evidence for apoptotic cell response and differential signals in chromatin condensation and DNA cleavage in victorin-treated oats. *The Plant Journal* **28,** 13–26.

Yao N, Tada Y, Sakamoto M, Nakayashiki H, Park P, Tosa Y, Mayama S. 2002. Mitochondrial oxidative burst involved in apoptotic response in oats. *The Plant Journal* **30,** 567–579.

Yin LN, Mano JC, Wang SW, Tsuji W, Tanaka K. 2010. The involvement of lipid peroxide-derived aldehydes in aluminium toxicity of tobacco roots. *Plant Physiology* **152,** 1406–1417.

Zhang LR, Xing D. 2008. Methyl jasmonate induced production of reactive oxygen species and alterations in mitochondrial dynamics that precede photosynthetic dysfunction and subsequent cell death. *Plant and Cell Physiology* **49,** 1092–1111.

Zhang LR, Xu QX, Xing D, Gao CJ, Xiong HW. 2009. Real-time detection of caspase-3-like protease activation *in vivo* using fluorescence resonance energy transfer during plant programmed cell death induced by ultraviolet C overexposure. *Plant Physiology* **150,** 1773–1783.

Zheng K, Pan JW, Ye L, *et al*. 2007. Programmed cell death-involved aluminium toxicity in yeast alleviated by antiapoptotic members with decreased calcium signals. *Plant Physiology* **143,** 38–49.